Solar Energy Materials and Solar Cells 29 (1993) 37–49
North-Holland

Solar Energy Materials and Solar Cells

Ray tracing analysis of the inverted pyramid texturing geometry for high efficiency silicon solar cells

A.W. Smith and A. Rohatgi

School of Electrical Engineering, Georgia Institute of Technology, Atlanta, GA 30332, USA

Received 15 May 1992; in revised form 16 September 1992

Various texturing schemes to trap weakly absorbed light into solar cells have been proposed. Light trapping in indirect band gap solar cells is necessary to increase the photogenerated current, thereby increasing the efficiency. Several common texturing geometries (slats, pyramids) have been examined to determine their light trapping characteristics. However, a detailed analysis of the geometry which produces the highest efficiency cells, the inverted pyramids, has not been reported. A quantitative analysis of the internal and external light trapping characteristics of the inverted pyramid geometry is presented for the first time. The internal characteristics show that the inverted pyramid geometry is able to confine the light better than the slats or upright pyramid designs, but possesses slightly poorer light trapping efficiency compared to a Lambertian front surface design. The path length enhancement for the inverted pyramid design is calculated to be ≈ 1.40 (as compared to a planar cell) which is superior to that of the slat (≈ 1.13) and pyramid (≈ 1.30) designs. The short wavelength spectral response analysis indicates that $\approx 37\%$ of the incoming light experiences a triple bounce on the front surface of the inverted pyramid geometry, while no rays experience a triple bounce in the slat and upright pyramid geometries. The superior internal response coupled with the path length enhancement and reduced front surface reflectance makes inverted pyramids an attractive and efficient single sided geometric light trapping geometry.

1. Introduction

Texturing solar cell surfaces to improve the cell performance has been attempted since 1960 [1]. There are three major objectives to light trapping by texturing the cell: (a) reduce the front surface reflectance, (b) increase the path length of the light through the cell, and (c) increase the amount of trapped light, reflected from the back surface, by total internal reflection at the front surface/air interface by making the incident angle greater than the critical angle. Current ray tracing analyzes concentrate on the path length enhancement and internal characteristics [2,3]. However, examination of the these two effects does not totally characterize the light trapping capabilities of a particular geometry. The light

Correspondence to: A.W. Smith, Georgia Tech Research Institute, Georgia Institute of Technology, Atlanta, GA 30332, USA.

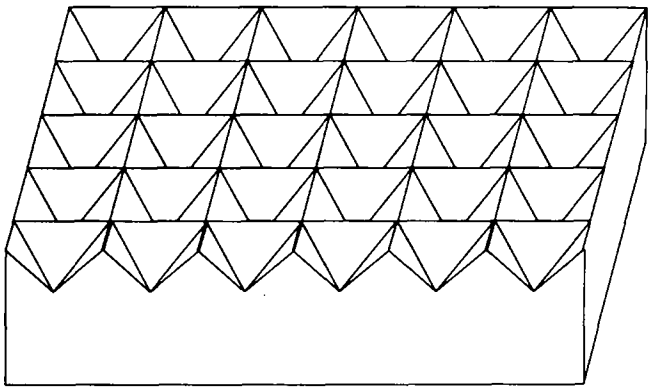

Fig. 1. The inverted pyramids geometry used for light trapping on the highest efficiency silicon solar cells.

trapping geometry which has been utilized on the highest efficiency cells [4,5], inverted pyramids, has not yet been analyzed in terms of the three criteria listed above.

The purpose of this paper is to examine all three aspects of light trapping in the inverted pyramid geometry shown in fig. 1. The properties of the inverted pyramids will be compared to the slats, pyramids, and Lambertian geometries to highlight the advantages and disadvantages of the geometry. First, the maximum current as a function of texturing angle and front surface reflectance is calculated. A spectral response argument for the increase in current as a function of texture angle is then formulated. The short wavelength spectral response, assuming 100% collection efficiency, is indicative of the number of bounces a ray undergoes on the front surface before being reflected away from the cell, reflection is the dominant loss mechanism. Comparison of the short wavelength spectral response at the natural texturing angles (53.75°) for the geometries shows the superior overall reflectance properties of the inverted pyramids. The internal characteristics and path length enhancement of all the geometries are calculated to support the improvement in current for the inverted pyramids. The maximum current as a function of cell thickness is then illustrated for Lambertian and inverted pyramid geometries with a double layer AR coating on the front surface. Finally, estimates of cell efficiencies are presented to show the potential of the inverted pyramids geometry.

2. Ray tracing program and material parameters

TEXTURE [6,7], a Monte Carlo ray tracing program was used extensively in this paper for the characterization and calculation of the light trapping efficiency for the surface structures. Two of the four output modes (quantitative and qualitative) are used in the analysis presented here.

In the quantitative mode, the program calculates the percentage of photons absorbed at each wavelength simulated. This is equivalent to the idealized spectral response with 100% internal quantum efficiency. From the knowledge of the front surface reflection coefficient and the percentage of photons absorbed at short wavelengths, the number of bounces on the front surface may be estimated. For instance, if the front surface reflectance ($R < 1$) is 30% and 97.3% of the photons are absorbed (A) then the rays of light must undergo a triple bounce before being reflected away from the cell ($A = 1 - R^3$). The quantitative mode also provides the total number of photons absorbed, multiplying this number by the electronic charge (q) gives an estimate of the maximum short circuit current assuming 100% collection of the photogenerated carriers. The increase in average surface area relative to a planar cell is also calculated in this mode to aid in estimating the change in open circuit voltage and efficiency of the textured cells following the analysis of Roedel and Holm [8]. In addition, the program calculates the number of photons not absorbed in the semiconductor due to losses out the sides of the cell and those lost at the back surface due to imperfect reflector.

In the qualitative mode, the program simulates the percentage of rays remaining as a function of the number of passes through the cell, the quantitative information about photon absorption is absent. As a texturing geometry becomes more efficient in trapping light by total internal reflection, a higher percentage of rays remain for the same number of passes through the cell. The qualitative mode also provides the average path length, relative to the thickness of a planar cell, to indicate the path length enhancement of the texturing scheme. Therefore, by a judicious use of the two output modes of the program all three important aspects (front surface reflectance, path length enhancement, internal reflection characteristics) of a texturing geometry can be examined.

Since texturing is more common for silicon solar cells as compared to the cells fabricated on III–V and II–VI materials, all the analysis and calculations in this paper are performed assuming Si cells. In the qualitative mode the back surface reflectance is automatically set to unity and the front surface reflectance is set to zero, to determine the internal trapping characteristics. Since no information on photon absorption is provided, the absorption coefficient of the material is not necessary. However, for the quantitative mode the input values for the index of refraction and absorption coefficients as a function of wavelength were obtained by importing the appropriate files from PC-1D version 3, a device modelling program [9]. In the quantitative mode the back surface reflectance was set to 98% for all wavelengths, unless specified differently. For the simulation of the absorbed flux, three different front surface reflection coefficients were used. In the first case, the reflectance was static at 30% to simulate bare Si. For the other two cases, files of front surface reflection as a function of wavelength were created to match a single layer anti-reflection (AR) coating of 70 nm of Si_3N_4 and a double layer AR coating consisting of 85 nm MgF and 50 nm of ZnS with a 5 nm SiO_2 passivation layer underneath, fig. 2. The light intensity simulated was 0.1 W/cm^2 with a spectral distribution corresponding to air mass 1.5. The AM1.5 direct spectrum file was imported from PC-1D version 3. The substrate thickness was assumed to be

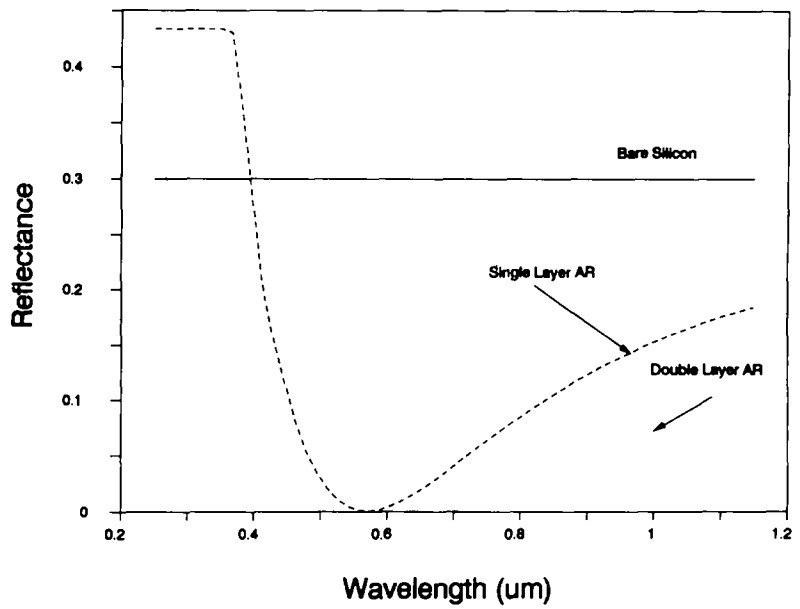

Fig. 2. Front surface reflectance as a function of wavelength for a single and double layer anti-reflection coatings, a static value of 30% is taken to represent bare silicon.

100 μm (unless specified otherwise), all of the texture heights were summed with the substrate thickness to produce the total cell thickness. The cell area was assumed to be 1 cm^2. The texture period was assumed to be 20 μm with face angles of 53.75°, except for the case when the texturing angle was varied. For the estimation of efficiency the cells considered had a conventional N^+PP^+ design using a 100 Ω cm substrate with an emitter depth of 0.2 μm and a surface concentration of 2.0×10^{19} cm^{-3}. The back surface diffusion was 2.0 μm with a surface concentration of 2.0×10^{18} cm^{-3}. Both diffusions were assumed to have the shape of the complementary error function. The minority carrier lifetime in the base was fixed at 2 ms, to provide collection of nearly all the photogenerated carriers and to model good quality material. The series resistance of the cell was set at 0.2 Ω and the surface recombination velocities were fixed at 5 cm/s for planar surfaces and 50 cm/s for Lambertian surfaces. This order of magnitude increase in surface recombination velocity may be extreme, but without the proper information these values seem reasonable. Planar and Lambertian cells of this design were simulated using PC-1D version 3. The solar cell parameters calculated from PC-1D for the planar cells were then used in the methodology of Roedel and Holm to estimate the efficiency of the textured cells. A two-dimensional analysis is avoided by assuming that all the photogenerated carrier are collected.

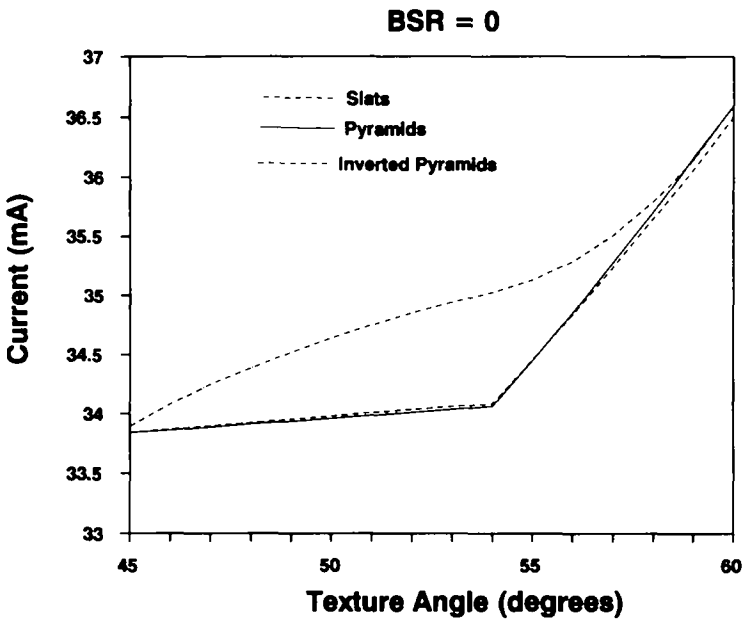

Fig. 3. Maximum current as a function of texturing angle for the slats, pyramids, and inverted pyramids designs on 100 μm cells. The front surface reflectance is set at 30% and no back surface reflector.

3. Results

Fig. 3 shows the calculated maximum current as a function of texturing angle for the three geometric texturing geometries (slats, pyramids; and inverted pyramids) with bare silicon front surface ($R = 30\%$) condition and no back surface reflector (0% reflection). At 45° and 60° all three geometries produce approximately the same maximum current. Examination of the short wavelength spectral response, fig. 4, indicates that at 45° the percentage of photons absorbed is indicative of a double bounce ($SR = 1 - R^2$) for all of the texturing geometries. At texturing angles of 60° the spectral response indicates that all of the rays undergo a triple bounce ($SR = 1 - R^3$) on the front surface before being reflected away. The small variations in current at texturing angles of 45° and 60° for the three different geometries are due to slight differences in the optical path length. For texturing angles between 45° and 60° the spectral response of the inverted pyramid geometry increases more than the spectral responses of the slats or upright pyramid, fig. 4. A higher percentage of rays ($\approx 37\%$ at an angle of 54°) undergo a triple bounce due to interaction with the adjoining planes of the inverted pyramid. Fig. 5 shows the reflection of light in a slat of 53.75°, no rays which strike the surface have the possibility of experiencing a triple bounce. In the case of the inverted pyramids rays which strike one face reflect light onto an orthogonal plane, which then reflects the light onto the face complementary to the original point of impact, fig. 6. Due to the higher percentage of rays undergoing a triple bounce the spectral

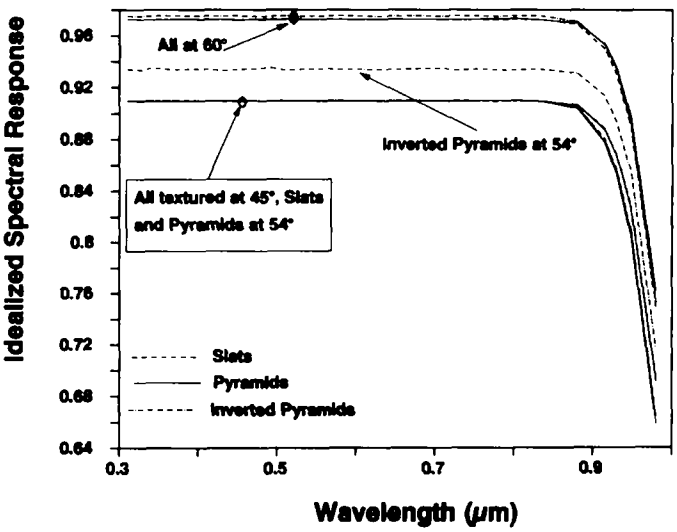

Fig. 4. Spectral response for the three cells depicted in fig. 3 at several texturing angles. The magnitude of the short wavelength response is indicative of the number of bounces on the front surface.

response of the inverted pyramids is higher than that of the slats or upright pyramids at texturing angles between 46° and 59°. The increase in spectral response has been shown to be valid for angles of incidence up to 10° off normal [7], although the spectral response is a complicated function of the angle of incidence. Fig. 7 shows the maximum current for the three geometric texturing geometries as a function of texturing angle and three front surface reflectance

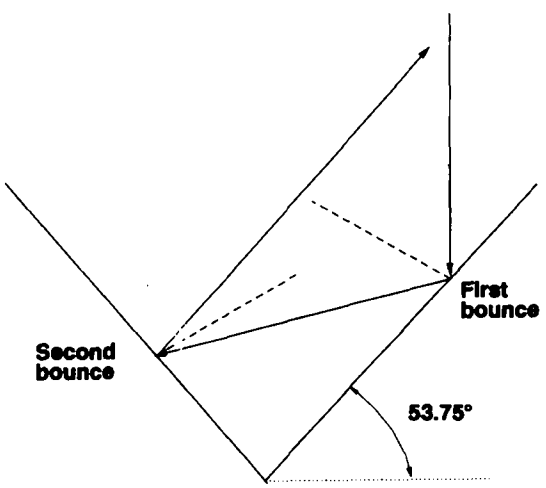

Fig. 5. Reflection of ray in slats with an angle to the horizontal of 53.75°, no rays are able to hit the surface three times, the same is true for the pyramids design.

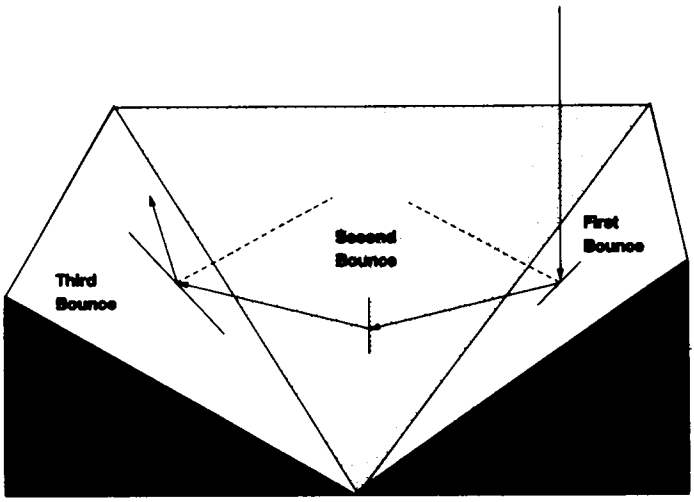

Fig. 6. Reflection of rays in the inverted pyramids design. Due to the impact of hitting an orthogonal plane a percentage of rays undergo a triple bounce on the front surface.

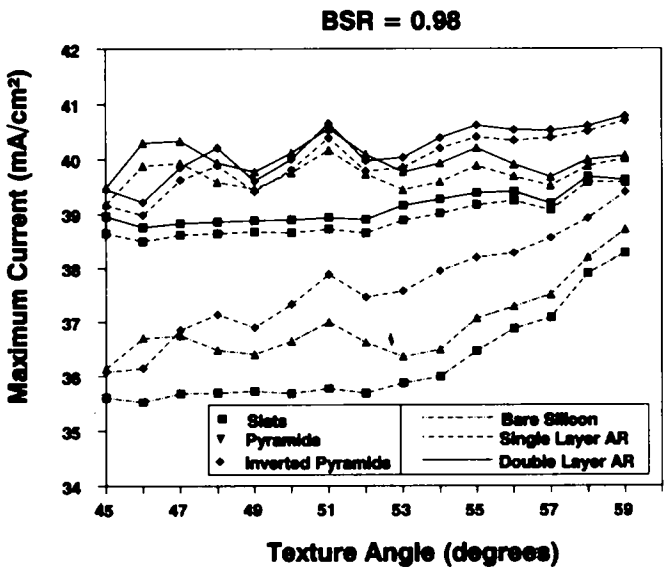

Fig. 7. Maximum current as a function of texturing angle for the slats, pyramids, and inverted pyramids designs on 100 μm cells. Three front surface reflectance conditions are shown, the back surface reflector was assumed to be 98% effective.

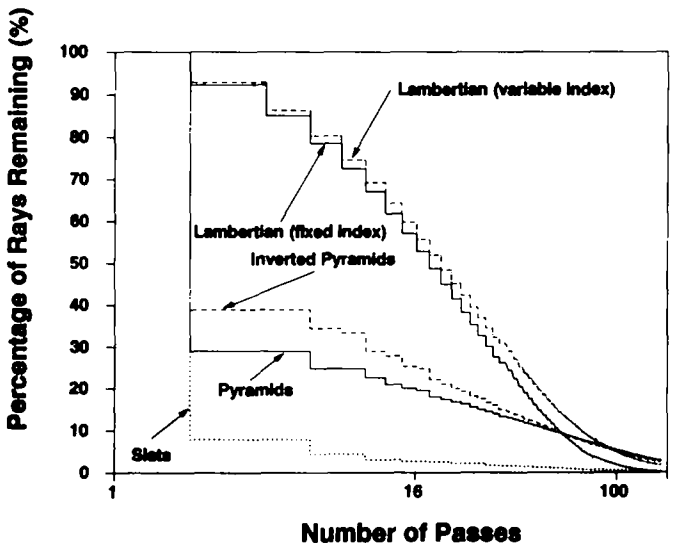

Fig. 8. Percentage of rays remaining as a function of the number of passes through the cell structure for: (a) Lambertian design with $\eta = 3.6$, (b) Lambertian design with variable η, (c) slats, (d) pyramids, and (e) inverted pyramids.

conditions, a 98% effective back surface reflector has been incorporated into the design. Notice the difference in the maximum current assuming bare silicon reflection condition for the three geometries as compared to fig. 3. This difference is due to the path length and internal light trapping characteristics which become important because of the application of the back surface reflector. Also from fig. 7, notice that as the front surface reflectance is decreased due to the application of AR coatings the importance of the triple bounce is diminished for the natural texturing angle of 53.75°, the difference in maximum current between the three geometries with AR coatings has become less.

The internal light trapping characteristics and path length enhancement, which have been included implicitly in fig. 7, of the three geometries will be compared to the characteristics of the Lambertian design. It has been well documented that the path length of the Lambertian design is approximately twice the substrate thickness (TEXTURE predicts 1.93). Also, the internal light trapping efficiency has been shown to be proportional to $1/\eta^2$ [2]. This proportionality dependence is depicted in fig. 8, assuming the index of refraction was fixed at 3.6. However, the simulations of the three geometries use index of refraction values which are a function of wavelength. Therefore, the comparison of the geometric geometries to the Lambertian case should be for the a variable index of refraction, which is also shown in fig. 8. The final three curves in fig. 8 show the percentage of rays trapped for the three geometric geometries, recall that there is no front surface reflectance and the back surface reflectance has been set to one. After 2 passes the inverted pyramids retains a higher percentage than either the pyramids or slats geometries.

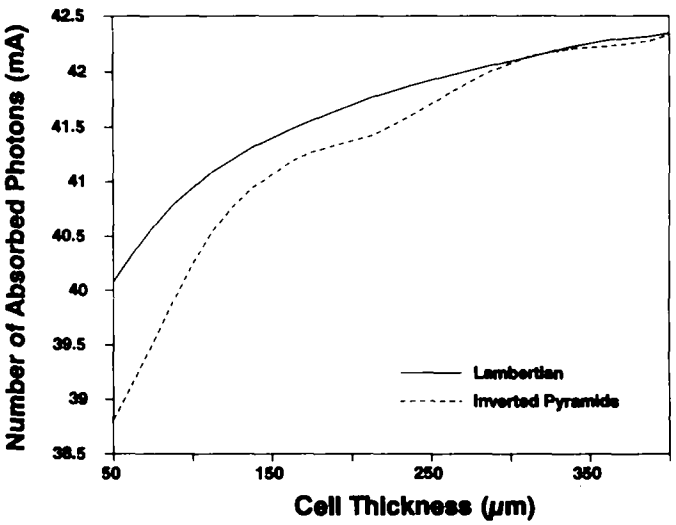

Fig. 9. Maximum current as a function of cell thickness for the Lambertian and inverted pyramids designs for three front surface reflectance conditions, the back surface reflector is 98% effective.

However, the percentage trapped by the inverted pyramids is much less than the Lambertian design. As previously stated the path length of the Lambertian design is approximately 2, while the inverted pyramid is 1.4073, this is superior to the slats and pyramids which have path length enhancements of 1.127 and 1.303, respectively.

Table 1
Calculated current values for inverted pyramids and Lambertian geometries with a double layer AR coating and 98% back surface reflector, all values in mA/cm^2.

Cell thickness (μm)	Inverted pyramids			Lambertian		
	J_{sc}	Back loss	Side loss	J_{sc}	Back loss	Side loss
50	38.8059	0.64706	0.03225	40.0823	1.2647	0.08216
75	39.5079	0.56089	0.04454	40.6128	1.1382	0.11107
100	40.2837	0.6586	0.06324	40.9639	1.0577	0.13709
125	40.8077	0.60283	0.08624	41.2250	0.99645	0.16308
150	41.0805	0.5906	0.06285	41.4072	0.9554	0.1990
175	41.297	0.66344	0.1237	41.5572	0.9161	0.2328
200	41.6577	0.6773	0.14501	41.7116	0.8758	0.2612
225	41.4862	0.5597	0.08460	41.8289	0.8458	0.2771
250	41.7255	0.5372	0.11483	41.9283	0.82098	0.28182
275	41.9170	0.5388	0.09983	42.0170	0.80066	0.30516
300	42.0933	0.4700	0.11711	42.0969	0.7863	0.3128
325	42.1862	0.48868	0.1205	42.1660	p.7699	0.33156
350	42.226	0.4825	0.2480	42.2280	0.7474	0.34716
375	42.2285	0.4959	0.18798	42.2897	0.7336	0.3422
400	42.3242	0.5494	0.1374	42.3426	0.7225	0.3475

The maximum current as a function of cell thickness is shown in fig. 9 and given in table 1 for the Lambertian and inverted pyramid designs assuming a double layer AR coating. As the thickness of the cell increases the difference in the predicted current between the two geometries decreases. Table 2 also contains the number of photons (in terms of current) lost due to the imperfect rear reflector (recall that it is only 98% effective) and finite cell dimensions. The magnitude of these losses is fairly small, but no longer insignificant.

4. Estimates of cell efficiency

The methodology of Roedel and Holm [8] was used to estimate the texture-induced improvement in cell efficiency and the degradation in open circuit voltage compared to the corresponding planar cell. In this methodology, the open circuit voltage of the textured cell (V_{oc}^{T}) is expressed as

$$V_{oc}^{T} = V_{oc}^{f} + \frac{KT}{q} \ln\left(\frac{1 + \left(J_{sc}^{T} - J_{sc}^{f}\right)/J_{sc}^{f}}{\text{Area}^{T}/\text{Area}^{f}} \right), \tag{1}$$

where V_{oc}^{f}, Area^{f}, J_{sc}^{f} are the open circuit voltage, surface area, and short circuit current of the planar cell, Area^{T} and J_{sc}^{T} are the area and calculated short circuit

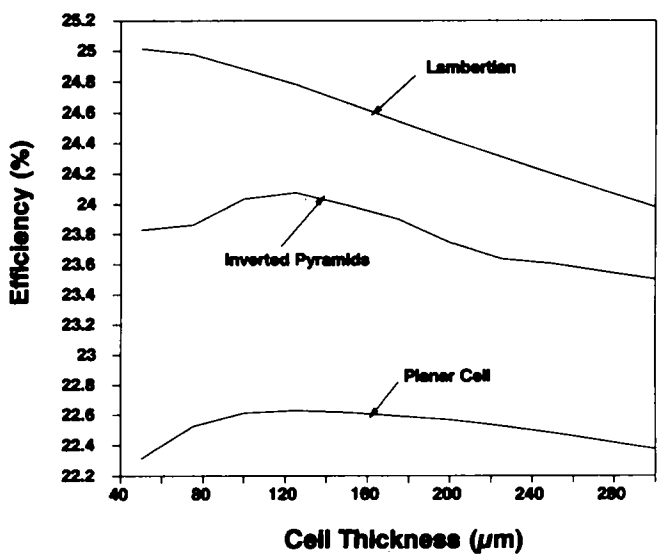

Fig. 10. Efficiency estimates for as a function of cell thickness for the planar, inverted pyramids, and Lambertian texturing geometries. The double layer AR coating reflectance was assumed for the front surface reflectance condition.

Table 2
Calculated solar cell parameters for planar, inverted pyramids, and Lambertian textured surfaces. Current is in mA/cm^2, voltage in V, and efficiency in 1%. All cells have double layer AR coating and 98% effective back surface reflector

Cell thickness (μm)	Planar cells			Inverted pyramids			Lambertian		
	J_{sc}	V_{oc}	η	J_{sc}	V_{oc}	η	J_{sc}	V_{oc}	η
50	35.8187	0.744874	22.31259	38.8059	0.733362	23.82858	40.0502	0.74671	25.01582
75	36.741	0.738296	22.52574	39.5079	0.72659	23.86497	40.6171	0.74009	24.97873
100	37.3415	0.733071	22.61292	40.2837	0.721449	24.03613	40.9827	0.734843	24.88188
125	37.78865	0.72872	22.62893	40.8077	0.717125	24.07675	41.24757	0.73047	24.78355
150	38.1458	0.72498	22.61687	41.0805	0.713313	23.99292	41.4526	0.726705	24.66462
175	38.4431	0.721689	22.59118	41.297	0.709957	23.90105	41.6186	0.723388	24.54479
200	38.6976	0.718741	22.56843	41.3577	0.706877	23.74727	41.7572	0.720419	24.42655
225	38.9194	0.716068	22.5271	41.4862	0.704136	23.63745	41.8757	0.717721	24.31113
250	39.11537	0.713618	22.48033	41.7255	0.701705	23.60516	41.9789	0.715248	24.19875
275	39.2902	0.711355	22.42951	41.91704	0.699445	23.55357	42.07	0.712962	24.08927
300	39.4473	0.709249	22.37562	42.09333	0.697345	23.50097	42.1514	0.710842	23.9825

current of the corresponding textured cell. The change in efficiency due to the textured surface (η^T) is then estimated from

$$\eta^T = \eta^f + \eta^f\left(\frac{\Delta J_{sc}}{J_{sc}^f} + \frac{\Delta V_{oc}}{V_{oc}^f}\right), \tag{2}$$

where η^f denotes the value of the efficiency for the planar cell, $\Delta V_{oc} = V_{oc}^T - V_{oc}^f$, and $\Delta J_{sc} = J_{sc}^T - J_{sc}^f$. The surface area ($\text{Area}^T$) and short circuit current (J_{sc}^T) for the textured cells were obtained from the output of the TEXTURE program. Using values of efficiency, open circuit voltage, and short circuit current for planar cells, calculated from PC-1D version 3, with eqs. (1) and (2) provide estimates of textured cell efficiencies assuming that the dominate recombination mechanism is area dependent. The results of the PC-1D calculations and estimates for inverted pyramids and Lambertian textured cells of various thicknesses are summarized in table 2 and fig. 10. Experimental values of current (42.9 mA/cm^2) from cells with the inverted pyramids geometry have been reported in ref. [5], correcting these values by 4% to 5% due to calibration error [10] puts the actual current in the range from 40.75 to 41.18 mA/cm^2. Model calculations for a substrate of comparable thickness predicted a current of 41.7 to 42.0 mA/cm^2, which is in good agreement with the experimental numbers considering grid coverage and global spectrum were not included in the simulation.

5. Conclusions

The light trapping properties of the inverted pyramid geometry has been analyzed for the first time. The increase in current for this type of textured cell is due to the incorporation of all three effects necessary for an efficient light trapping design. The front surface reflectance is reduced by providing the opportunity for a portion of the incoming light to undergo a triple bounce, thereby reducing the overall front surface reflectance. The increase in path length and light trapping efficiency means that a larger fraction of the light which has entered the cell will be absorbed before exiting the cell. It is shown quantitatively for the first time that the inverted pyramids geometry is superior to either the slats or regular pyramids. The inverted pyramids on a 100 μm cell with a two layer AR coating is estimated to give 40.2 mA/cm^2 and cell efficiencies of $\approx$ 24% with realistic cell design and material parameters.

References

[1] B. Dale and H.G. Rudenberg, Proc. of the 14th Annual Power Sources Conf., U.S. Army Signal Research and Development Lab. (1960) p. 22.
[2] P. Campbell and M.A. Green, J. Appl. Phys. (1987) 243.
[3] M.A. Green and P. Campbell, in Proc. of the 19th IEEE Photovoltaic Specialist Conf. (IEEE, New York, (1987) pp. 912–917.

[4] A. Cuevas, R.A. Sinton, and R.M. Swanson, Proc. of the 21st IEEE Photovoltaic Specialist Conf. pp. 327–332.
[5] N. Zhao, A. Wang and M.A. Green, Proc. of the 21st IEEE Photovoltaic Specialist Conf. pp. 333–335.
[6] A.W. Smith, A. Rohatgi, and S.C. Neel, Proc. of the 21st IEEE Photovoltaic Specialist Conf. (IEEE, New York, 1990) pp. 426–431.
[7] A.W. Smith, Ph.D. dissertation, Georgia Institute of Technology, Atlanta, GA, 1992.
[8] R.J. Roedel and P.M. Holm, Sol. Cells 11 (1987) 221.
[9] P.A. Basore, PC-1D Installation Manual and User's Guide Version 3.0, Sandia National Laboratories, Albuquerque, NM (1991).
[10] J. Gee, Sandia National Laboratories, private Communication (1990).